Available online at www.sciencedirect.com

SciVerse ScienceDirect

Ceramics International 39 (2013) 8097–8101

CERAMICS INTERNATIONAL

www.elsevier.com/locate/ceramint

Improved efficiency of dye-sensitized solar cells through fluorine-doped TiO_2 blocking layer

Suk In Noh[a], Kokn-Nara Bae[a], Hyo-Jin Ahn[b,*], Tae-Yeon Seong[a,*]

[a]*Department of Materials Science and Engineering, Korea University, Seoul 136-713, Republic of Korea*
[b]*Department of Materials Science and Engineering, Seoul National University of Science and Technology, Seoul 139-743, Republic of Korea*

Received 21 March 2013; received in revised form 25 March 2013; accepted 25 March 2013
Available online 6 April 2013

Abstract

We report on improvement in the performance of dye-sensitized solar cells (DSSCs) through a fluorine (F)-doped TiO_2 dense layer for use as a blocking layer. The F-doped TiO_2 layer was deposited on commercial F-doped SnO_2 (FTO) substrate by the hydrolysis of a $TiCl_4$ aqueous solution with NH_4F. Their structural, morphological, and optical properties were investigated by scanning electron microscopy (SEM), X-ray diffraction (XRD), X-ray photoelectron spectroscopy (XPS), and UV–vis spectroscopy examinations. The photocurrent density–voltage characteristics show that DSSCs fabricated with the F-doped TiO_2 layer exhibits higher conversion efficiency (~5.24%) than ones with the undoped TiO_2 layer (~4.76%), and the bare FTO substrate (~3.88%). This improvement is attributed to the combined effects of reduced interfacial resistance and effective blocking behavior by the F-doped TiO_2 dense layer.

Keywords: Dye-sensitized solar cell; F-doped TiO_2; Interfacial resistance; Blocking layer

1. Introduction

Dye-sensitized solar cells (DSSCs) have been regarded as a good alternative to silicon solar cells because of their advantages, such as low manufacturing cost, less toxic production environment, and various industrial applications [1,2]. Generally, DSSCs usually consist of a nanoporous TiO_2 layer deposited onto F-doped SnO_2 (FTO) glass (working electrode), photo-energy absorbing dye molecules, I^-/I_3^- electrolyte, and a Pt-coated FTO glass (counter electrode) [3]. For the conventional DSSCs, the nanoporous TiO_2 layer provides not only large surface areas for dye loading, but also recombination sites, such as the TiO_2/electrolyte and FTO/electrolyte interfaces in the working electrode [4]. This could cause back-electron transfer from the conduction band of the TiO_2 to the redox level of I^-/I_3^- electrolyte and the HOMO level of Ru-dye. In particular, retarding the recombination at the interface between the FTO glass surface and the electrolyte have received great attention for the high-efficiency DSSCs [5]. Thus, in an attempt to prevent the back electron transfer, a dense TiO_2 layer was employed between the FTO glass and nanoporous TiO_2 layers [6–8]. However, the inserted dense TiO_2 layer showed non-ohmic behavior between the nanoporous TiO_2 layer and the FTO glass [9]. Although considerable efforts were made to develop high-quality blocking layers for use in DSSCs, works on the fabrication of efficient blocking layers having low interfacial resistance have not been extensively done so far. For example, Lee et al. deposited an Nb-doped TiO_2 dense layer on the FTO glass by pulsed laser deposition so as to form ohmic contacts [10]. However, the Nb-doped TiO_2 layer yielded high conductivity only when deposited on the $SrTiO_3$ substrate [11]. Moreover, non-metallic element-doped TiO_2 layers have advantages, such as thermal stability and low cost (lower than Nb) [12]. Thus, in this work, F-doped TiO_2 dense layers were introduced between FTO glass and nanoporous TiO_2 electrode by a hydrolysis method to form a blocking layer having low interfacial resistance. In other words, we investigated the effect of an F-doped TiO_2 blocking layer on the performance of DSSCs.

2. Experimental procedure

2.1. Sample preparation

The FTO glass (8 Ω/□, Pilkington) substrates for depositing undoped and F-doped TiO_2 dense layers were sequentially

*Corresponding authors. Tel.: +82 2 3290 3288; fax: +82 2 928 3584.
E-mail addresses: hjahn@seoultech.ac.kr (H.-J. Ahn), tyseong@korea.ac.kr (T.-Y. Seong).

0272-8842/$ - see front matter © 2013 Elsevier Ltd and Techna Group S.r.l. All rights reserved.
http://dx.doi.org/10.1016/j.ceramint.2013.03.082

cleaned with acetone, methanol, and DI water. The FTO substrate was then immersed into a 40 mM $TiCl_4$ (Titanium (IV) chloride, Aldrich) solution at 80 °C for 30 min to deposit a undoped TiO_2 layer. The F-doped TiO_2 layer was deposited on the FTO substrate from the hydrolysis of $TiCl_4$ with 10 at% of NH_4F (Ammonium fluoride, Aldrich). The samples were rinsed with ethanol and then annealed at 450 °C for 30 min. The layer thicknesses were measured to be 70 ± 5 nm by an Alpha step profiler (Nanomap-LS).

To form TiO_2 paste, TiO_2 nanoparticles (Degussa, P25) (16.2 wt%) were dispersed into DI water (67.5 wt%) with HPC (Aldrich) (11.9 wt%) and Acetyl acetone (Aldrich) (4.4 wt%), and then ground using Al_2O_3 mortar for 4 h. The TiO_2 paste was then coated onto the F-doped TiO_2 and undoped TiO_2 dense layers (0.25 cm^2 in size) on the FTO glass substrates by squeeze printing, followed by sintering at 500 °C for 1 h. For dye adsorption, the sintered samples were immersed into a 0.5 mM $Ru(dcbpy)_2(NCS)_2$ (N719, Solaronix) solution for 24 h in a dark room and washed with ethanol. The Pt electrode was prepared by a drop coating method onto the FTO glass using a 5 mM $H_2PtCl_6 \cdot 6H_2O$ (Aldrich) solution in isopropanol and then sintered at 450 °C for 30 min. An iodine electrolyte based on 0.3 M BMII was used [13].

2.2. Characterization

The morphologies of the samples were assessed by field-emission scanning electron microscopy (FESEM, Hitachi SU70) and atomic force microscopy (AFM, XE-100). The structural properties were characterized by X-ray diffraction (XRD, Bruker D8-Advance with Cu K_α radiation) and X-ray photoelectron spectroscopy (XPS, Axis-His-corrected by the reference C 1*s* peak with 284.5 eV). The optical properties were examined by UV–vis spectrophotometer (Shimadzu, UV-1800). The photocurrent–voltage curves of DSSCs were investigated under standard irradiance (AM 1.5 simulated sunlight) using a 150 W xenon lamp (LAB 50).

3. Results and discussion

Fig. 1 shows SEM images obtained from bare and TiO_2-coated FTO glass substrates. Unlike the bare FTO glass

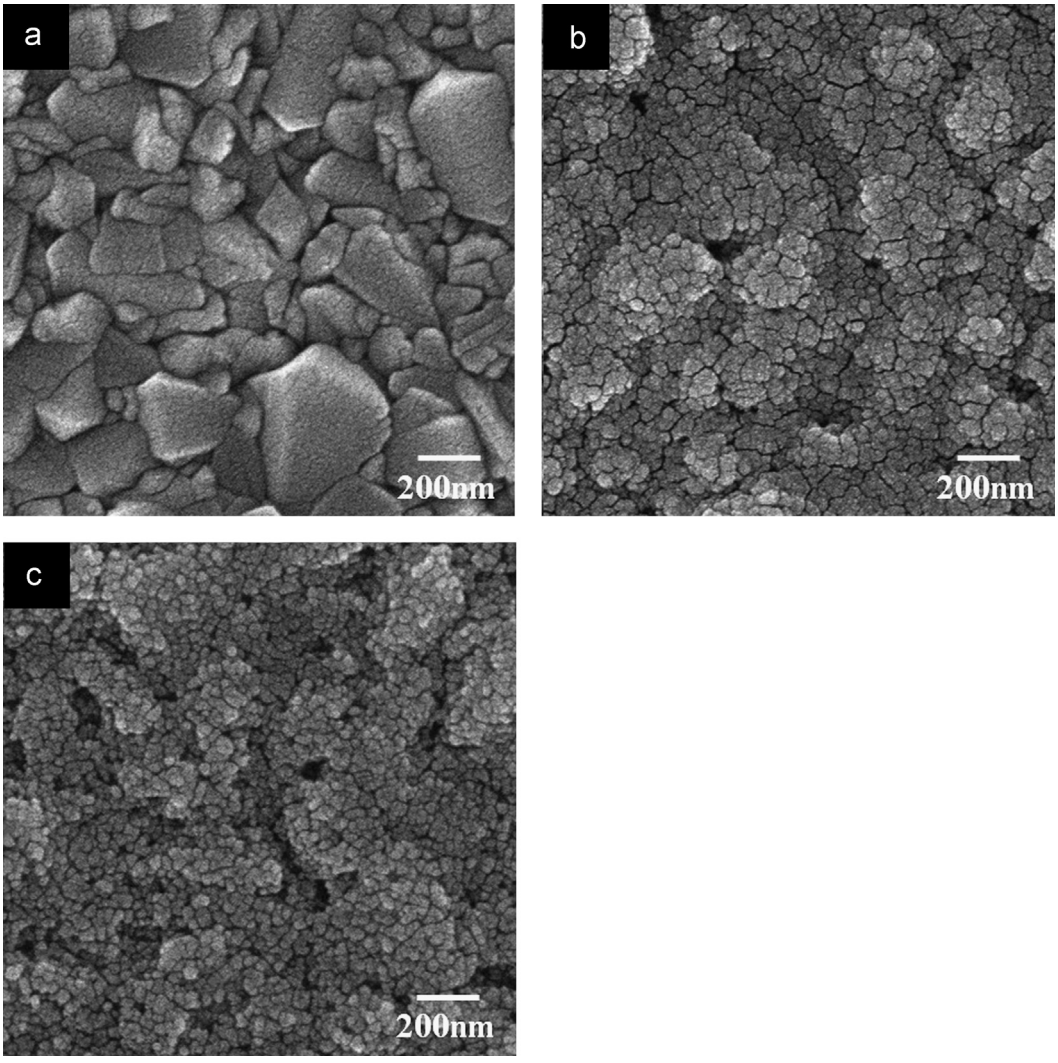

Fig. 1. SEM images obtained from (a) bare FTO glass, (b) undoped TiO_2 layer and (c) F-doped TiO_2 layer.

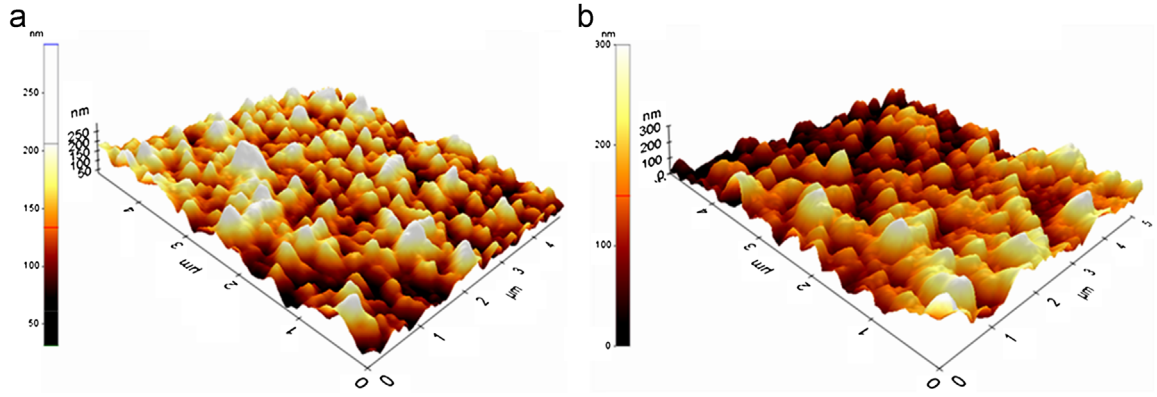

Fig. 2. AFM images of (a) undoped TiO_2 layer and (b) F-doped TiO_2 layer.

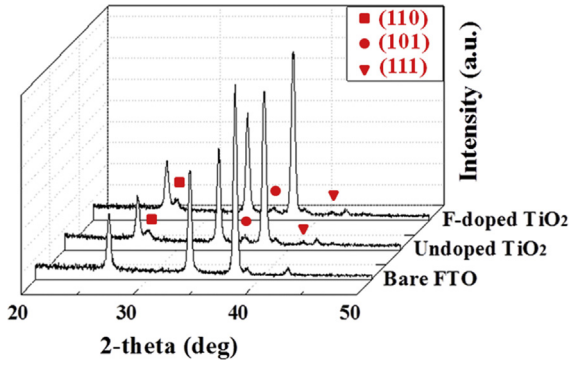

Fig. 3. XRD plots for bare FTO glass, undoped TiO_2 layer and F-doped TiO_2 layer.

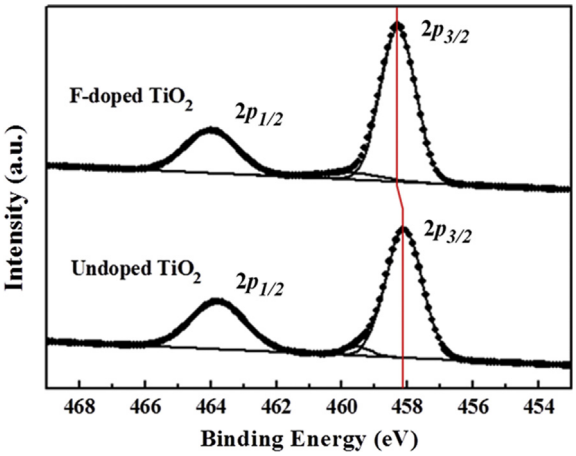

Fig. 4. XPS Ti 2p core level spectra from undoped and F-doped TiO_2 layers.

(Fig. 1(a)), the TiO_2-coated FTO substrates consist of small grains. For the undoped TiO_2 dense layer, the grains vary from ~17 to 75 nm in size (Fig. 1(b)), while the F-doped TiO_2 dense layer contains grains in the range ~5–30 nm (Fig. 1(c)). Furthermore, the F-doped TiO_2 layer shows a somewhat rougher surface than the undoped TiO_2 layer. The AFM results (Fig. 2) showed that the root-mean square (RMS) roughness is 33.8 and 76.1 nm for the undoped and F-doped samples, respectively. It is noted that the F-doping causes a roughening of the surface of the TiO_2 layers.

Fig. 3 exhibits XRD plots for the bare and TiO_2-coated FTO glass substrates. In addition to the diffraction peaks from the FTO glass, the undoped TiO_2 sample reveals peaks at 27.4°, 36.0°, and 41.2°, corresponding to the (110), (101), and (111) planes of rutile TiO_2 (JCPDS no. 21-1276). The F-doped TiO_2 sample exhibits the same peaks. It means that the phase transition has not occurred by F-doping. Thus, the different performance of DSSCs is not attributed to the changes of phase.

Fig. 4 shows the XPS Ti 2p core level spectra from the TiO_2 dense layers with and without F-doping. The Ti $2p_{3/2}$ core level peak is observed at ~458.14 eV and ~458.36 eV for the undoped and F-doped samples, respectively. Notably, the Ti 2p core level for the F-doped TiO_2 sample shifts toward the higher binding-energy side by 0.22 eV compared to that of the undoped sample. This could be due to the fact that F atom has lower electronegativity than oxygen atom [14].

Fig. 5(a) shows the transmittance of the bare and TiO_2-coated FTO glass substrates. At an effective region for photo-energy conversion (namely, at 550 nm), the F-doped TiO_2 layer exhibits a transmittance of 70.8%, whereas the undoped TiO_2 layer shows only 66.5%. Fig. 5(b) exhibits the absorption coefficients of the TiO_2 samples, which were obtained from Fig. 5(a). The transmittance is given as

$$I = I_o e^{-\alpha t} \quad (1)$$

where I and I_o is the intensity of transmitted and incident light, respectively, α is the absorption coefficient, and t is the thickness (70 nm). Since the transmittance in an indirect semiconductor is described as I/I_o, the relation between α and optical energy bandgap (E_g) is given as

$$\alpha = (h\nu - E_g)^2 \quad (2)$$

where h is the Planck constant, and ν is the frequency of incident photon. Then, the optical bandgap (E_g) is determined by an extrapolation method, namely, a value at which $\alpha^{1/2}$ is zero [15]. The extrapolation showed that the optical bandgap was ~3.56 and ~3.81 eV for the undoped and F-doped TiO_2 layers, respectively. A comparison shows that the F-doping causes a shift of the surface Fermi level toward the higher-energy side, being indicative of degenerated F-doped TiO_2. This is consistent with the high-energy side shift of the Ti 2p

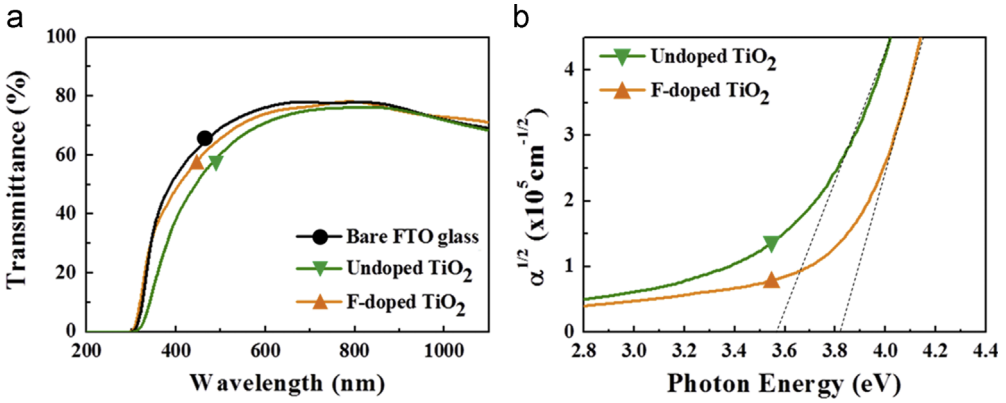

Fig. 5. (a) Transmittance of bare FTO glass, undoped TiO_2 layer and F-doped TiO_2 layer. (b) The absorption coefficients of undoped and F-doped TiO_2 samples as a function of photon energy.

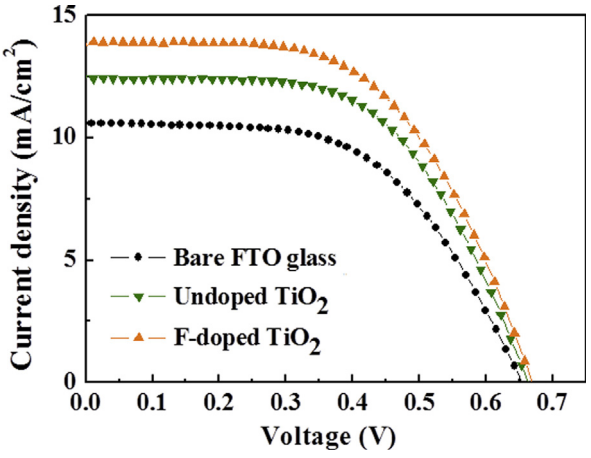

Fig. 6. Photocurrent density–voltage characteristics of DSSCs fabricated with bare and TiO_2-coated FTO glass substrates.

Table 1
Photovoltaic properties of DSSCs fabricated with bare and TiO_2-coated FTO glass substrates.

Samples	J_{sc} [mA/cm^2]	V_{oc} [V]	*ff*	η [%]
Bare FTO glass	10.60	0.65	0.56	3.88
Undoped TiO_2	12.44	0.66	0.58	4.76
F-doped TiO_2	13.89	0.67	0.57	5.24

core level for the F-doped TiO_2 (Fig. 4). The work functions of the bare and TiO_2-coated FTO glass substrates were examined by a surface analyzer (AC-2, RIKEN). The work function was measured to be ~5.69, ~4.84, and ~4.48 eV for the FTO glass, undoped TiO_2 and F-doped TiO_2 layers, respectively, being consistent with the optical bandgap data. The degenerated n-type TiO_2 layer between the FTO glass substrate and the nanoporous TiO_2 layer is expected to form an ohmic contact [10], leading to the improved performance of DSSCs by reducing interfacial resistance.

Fig. 6 shows the photocurrent density–voltage characteristics of DSSCs fabricated with the bare and TiO_2-coated FTO glass substrates. Associated photovoltaic parameters are summarized in Table 1. The DSSCs with the undoped TiO_2 dense layer show ~17.4% higher current density, leading to ~22.6% better conversion efficiency than the cells with the bare FTO glass. This implies that the undoped TiO_2 dense layer effectively serves as a blocking layer. In case of the DSSCs with the F-doped TiO_2 dense layer, they show ~11.7% higher current density than the cells with the undoped TiO_2 dense layer, leading to ~10.1% enhanced conversion efficiency. This implies that the F-doped TiO_2 dense layer effectively serves as a blocking layer with reduced interfacial resistance through controlling band structure. In other words, the F-doped TiO_2 dense layer reduces the interfacial resistance by forming ohmic contact, causing efficient flow of electrons. Furthermore, the F-doped TiO_2 dense layer serves as an efficient blocking layer. These results imply that the F-doped TiO_2 dense layer could serve as a promising blocking layer for fabricating high-performance DSSCs.

4. Summary

F-doped TiO_2 dense layers were deposited onto FTO glass substrates by the hydrolysis of of $TiCl_4$ with 10 at% of NH_4F for use as a blocking layer. DSSCs fabricated with the F–TiO_2 dense layer exhibited higher photo-conversion efficiency than conventional DSSCs with an undoped TiO_2 dense layer. The improved performance was ascribed to the fact that the F-doped TiO_2 layer served as a blocking layer to prevent the back electron transfer and resulted in the reduced interfacial resistance.

Acknowledgments

This work was supported by the World Class University Program through the National Research Foundation of Korea funded by MEST (R33-2008-000–10025-0).

References

[1] B. O'Regan, M. Grätzel, A low-cost, high-efficiency solar cell based on dye-sensitized colloidal TiO_2 films, Nature 353 (1991) 737–740.
[2] S.I. Noh, H.J. Ahn, D.H. Riu, Photovoltaic property dependence of dye-sensitized solar cells on sheet resistance of FTO substrate deposited via spray pyrolysis, Ceramics International 12 (2012) 6065–6068.

[3] W. Yuqiao, S. Yueming, L. Kang, Dye-sensitized solar cells based on oriented ZnO nanowire-covered TiO_2 nanoparticle composite film electrodes, Materials Letters 63 (2009) 1102–1104.
[4] Y. Hua, Z. Shanqing, Z. Huijun, W. Geoffrey, L. Porun, An efficient and low-cost TiO_2 compact layer for performance improvement of dye-sensitized solar cells, Electrochimica Acta 54 (2009) 1319–1324.
[5] M. Wu, Z.H. Yang, Y.H. Ziang, J.J. Zhang, S.Q. Liu, Y.M. Sun, Improvement of dye-sensitized solar cell performance through electrodepositing a close-packed TiO_2 film, Journal of Solid State Electrochemistry 14 (2010) 857–863.
[6] N.G. Park, G. Schlichthorl, J. van de Lagemaat, H.M. Cheong, A. Mascarenhas, A.J. Frank, Dye-sensitized TiO_2 solar cells: structural and photoelectrochemical characterization of nanocrystalline electrodes formed from the hydrolysis of $TiCl_4$, Journal of Physical Chemistry B 103 (1999) 3308–3314.
[7] Y.J. Kim, Y.H. Lee, M.H. Lee, H.J. Kim, J.H. Pan, G.I. Lim, Y.S. Choi, K.K. Kim, N.G. Park, C.M. Lee, W.I. Lee, Formation of efficient dye-sensitized solar cells by introducing an interfacial layer of long-range ordered mesoporous TiO_2 thin film, Langmuir 24 (2008) 13225–13230.
[8] S. Ito, T.N. Murakami, P. Comte, P. Liska, C. Grätzel, M. K. Nazeeruddin, M. Grätzel, Fabrication of thin film dye sensitized solar cells with solar to electric power conversion efficiency over 10%, Thin Solid Films 516 (2008) 4613–4619.
[9] H.J. Snaith, M. Grätzel, The role of a Schottky barrier at an electron-collection electrode in solid-state dye-sensitized solar cells, Advanced Materials 18 (2006) 1910–1914.
[10] S.W. Lee, J.H. Noh, H.S. Han, D.K. Yim, D.H. Kim, J.K. Lee, J.Y. Kim, H.S. Jung, K.S. Hong, Nb-doped TiO_2: a new compact layer material for TiO_2 dye-sensitized solar cells, Journal of Physical Chemistry C 113 (2009) 6878–6882.
[11] T. Hitosugi, A. Ueda, S. Nakao, M. Yamada, Y. Furubayashi, Y. Hirose, T. Shimada, T. Hasegawa, Fabrication of highly conductive TiNbO polycrystalline films on glass substrates via crystallization of amorphous phase grown by pulsed laser deposition, Applied Physics Letters 90 (2007) 212106.
[12] R.S. Zhang, Y. Liu, Q. Gao, F. Teng, C.L. Song, W. Wang, G.R. Han, First-principles study on the electronic and optical properties of F-and Nb-doped anatase TiO_2, Journal of Alloys and Compounds 509 (2011) 9178–9182.
[13] S. Ito, P. Chen, P. Comte, M. Nazeeruddin, P. Liska, P. Péchy, M. Grätzel, Fabrication of screen-printing pastes from TiO_2 powders for dye-sensitised solar cells, Progress in Photovoltaics: Research and Applications 15 (2007) 603–612.
[14] J. Song, H.B. Yang, X. Wang, S.Y. Khoo, C.C. Wong, X.W. Liu, C. M. Li, Improved utilization of photogenerated charge using fluorine-doped TiO_2 hollow spheres scattering layer in dye-sensitized solar cells, ACS Applied Materials and Interfaces 4 (2012) 3712–3717.
[15] E. Ziegler, A. Heinrich, H. Oppermann, G. Stover, Electrical properties and non-stoichiometry in ZnO single crystals, Physica Status Solidi A 66 (1981) 635–648.